

## Tunable Chiral Reaction Media Based on Two-Component Liquid Crystals: Regio-, Diastereo-, and Enantiocontrolled Photodimerization of Anthracenecarboxylic Acids

Yasuhiro Ishida,<sup>\*,†,§</sup> Ammathnadu S. Achalkumar,<sup>†</sup> Shun-ya Kato,<sup>‡</sup> Yukiko Kai,<sup>‡</sup> Aya Misawa,<sup>‡</sup> Yumi Hayashi,<sup>‡</sup> Kuniyo Yamada,<sup>†</sup> Yuki Matsuoka,<sup>§</sup> Motoo Shiro,<sup>⊥</sup> and Kazuhiko Saigo<sup>‡,¶</sup>

RIKEN, Advanced Science Institute, 2-1 Hirosawa, Wako, Saitama 351-0198, Japan, Department of Chemistry and Biotechnology, Graduate School of Engineering, The University of Tokyo, Hongo, Bunkyo-ku, Tokyo 113-8656, Japan, PRESTO, Japan Science and Technology Agency, 4-1-8 Honcho, Kawaguchi, Saitama 332-0012, Japan, Rigaku Corporation, 3-9-12 Matsubara-cho, Akishima, Tokyo 196-8666, Japan, and School of Environmental Science and Engineering, Kochi University of Technology, Miyakouchi, Tosayamada-cho, Kami, Kochi 782-8502, Japan

Received June 17, 2010; E-mail: y-ishida@riken.jp

**Abstract:** Three kinds of enantiopure amphiphilic amino alcohols (**1a–c**) were newly synthesized, of which the stereochemistry of the stereogenic carbons adjacent to the amino (C2) and hydroxy (C1) groups was systematically varied. By using these amino alcohols and four photoreactive carboxylic acids, 12 kinds of salts were prepared. The structure and thermal behavior of the salts were thoroughly investigated by various techniques, which revealed that the stereochemistry of the amino alcohol unit has significant effects on the properties of the salts; the salts of **1a** with (1*R*,2*S*)-configuration did not exhibit any liquid crystal (LC) phase but showed high crystallinity, whereas **1b** and **1c** with (1*S*,2*S*)- and (1*S*)-configurations, respectively, generally afforded stable LC salts with smectic structure(s). Within the matrix of these amphiphilic salts, the in situ photodimerizations of 2-anthracenecarboxylic acid (**2c**) and 1-anthracenecarboxylic acid (**2d**) were conducted by the irradiation with UV/vis light (500 W, a high-pressure mercury arc lamp, >380 nm). Concerning reactivity and regio-/diastereo-/enantioselectivities, the LC phases were found to be superior to isotropic and crystalline phases. For the two substrates **2c** and **2d**, every LC phase promoted the photodimerization with unprecedentedly high *head-to-head* selectivity. Particularly in the case of **2c**, diastereoselectivity (*syn*<sup>HH</sup> vs *anti*<sup>HH</sup>) could be rationally controlled by the choice of the amino alcohol unit and mesophase (*syn*<sup>HH</sup>:*anti*<sup>HH</sup> = 61:37 to 26:72). Moreover, one of the LC phases exhibited by **1b·2c** afforded the *anti*<sup>HH</sup>-dimer of **2c** with excellent enantioselectivity (up to 86% ee). On the basis of the hypothesis that the present photochemical outcome arises from the preorientation of the substrates, a preliminary structural model of these LCs was proposed.

### 1. Introduction

There has been increasing interest in controlling the course of chemical reactions by using ordered media.<sup>1–6</sup> To date, a number of ordered reaction media have been explored, such as crystals,<sup>1</sup> coordination polymers,<sup>2</sup> zeolites,<sup>3</sup> clays,<sup>4</sup> discrete hosts in homogeneous solutions,<sup>5</sup> etc. These constrained reaction environments have attracted continuous attention as one of the simplest models of biological reaction systems. In addition, medium-controlled reactions might establish a practically useful methodology, which play a significant role complementary to traditional organic synthesis in homogeneous media. Particularly, precise stereocontrol of photochemical reactions has remained as an unexplored issue in the framework of homogeneous systems. For this purpose, ordered reaction media would offer great promise in preorganizing substrates to yield well-controlled

products. Despite such significance, however, the idea of medium-controlled reactions has an inherent limitation, a “trade-off” between selectivity and reactivity. As represented by crystalline reaction systems, extremely ordered media occasionally realize almost perfect reaction control, but in most cases, severe restriction on molecular motions fatally reduces the probability of reactions.<sup>1,2</sup> Contrary to crystals, supramolecular aggregates such as micelles,<sup>6</sup> physical gels,<sup>7</sup> bilayers,<sup>8</sup> etc. are

<sup>†</sup> RIKEN, Advanced Science Institute.

<sup>‡</sup> The University of Tokyo.

<sup>§</sup> PRESTO, Japan Science and Technology Agency.

<sup>⊥</sup> Rigaku Corporation.

<sup>¶</sup> Kochi University of Technology.

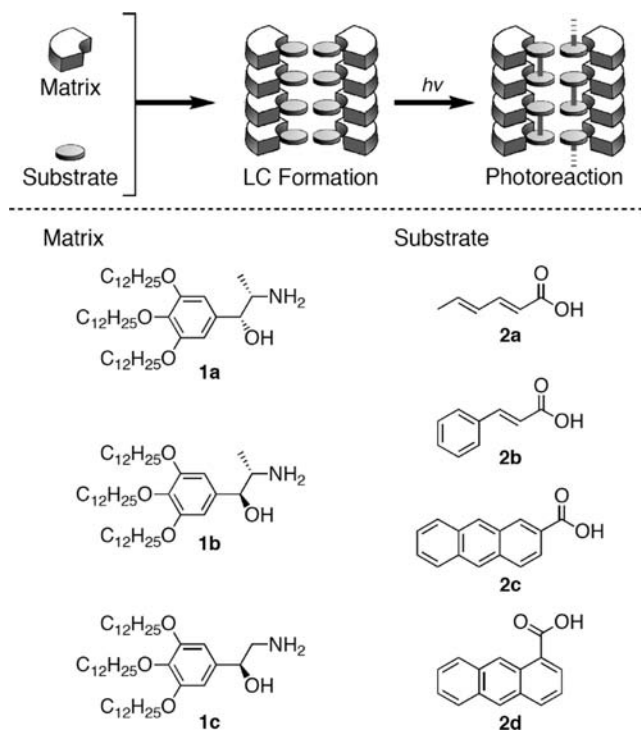
- (1) (a) Tanaka, K.; Toda, F. *Chem. Rev.* **2000**, *100*, 1025–1074. (b) Braga, D.; Grepioni, F. *Angew. Chem., Int. Ed.* **2004**, *43*, 4002–4011. (c) Matsumoto, A. *Top. Curr. Chem.* **2005**, *254*, 263–305.  
 (2) (a) Kitagawa, S.; Kitaura, R.; Noro, S. *Angew. Chem., Int. Ed.* **2004**, *43*, 2334–2375. (b) Georgiev, I. G.; MacGillivray, L. R. *Chem. Soc. Rev.* **2007**, *36*, 1239–1248.  
 (3) (a) Joy, A.; Ramamurthy, V. *Chem.—Eur. J.* **2000**, *6*, 1287–1293. (b) Tung, C.-H.; Wu, L.-Z.; Zhang, L.-P.; Chen, B. *Acc. Chem. Res.* **2003**, *36*, 39–47. (c) MacGillivray, L. R.; Papaefstathiou, G. S.; Friscic, T.; Varshney, D. B.; Hamilton, T. D. *Top. Curr. Chem.* **2004**, *248*, 297–310. (d) Kaupp, G. *Top. Curr. Chem.* **2005**, *254*, 95–183.  
 (4) (a) Varma, R. S. *Tetrahedron* **2002**, *58*, 1235–1255. (b) Georgakilas, V.; Gournis, D.; Bourlinos, A. B.; Karakassides, M. A.; Petridis, D. *Chem.—Eur. J.* **2003**, *9*, 3904–3908.

generally unable to realize ideal selectivity, although their relatively loose structures are promising to promote in situ reactions.

To solve the problem as described above, several groups have employed liquid crystals (LCs) as media to control chemical reactions.<sup>6a,9</sup> Among supramolecular aggregates, thermotropic LCs are regarded as one of the most structurally ordered classes, which should be advantageous for the control of organic transformations. Particularly, cholesteric LCs have been extensively studied as media for asymmetric reactions in the 1970's.<sup>10</sup> Nevertheless, most of the previous attempts have resulted in unsatisfactory selectivity, especially in terms of enantioselectivity, probably due to the following reasons: (1) the environment of photoreactive substrates is not necessarily "monoclonal" in these LC media, because the substrates are just mixed with chiral mesogenic components to weakly interact with them, and (2) in the attempts of enantiocontrol by cholesteric LC media, their helical structures (from 100 nm to  $\mu\text{m}$  pitch) seems to be too huge to bring a significant effect on events at a molecular level.<sup>11</sup>

On the other hand, our recent studies revealed that the salts of amphiphilic carboxylic acids with amines/amino alcohols have a high propensity to exist as thermotropic LCs in wide thermal ranges.<sup>12</sup> The promising results led us to expect that the opposite combinations, i.e. the salts of amphiphilic amino alcohols with carboxylic acids would have a similar tendency. If a photoreactive species is used as the carboxylic acid unit, its transformation is expected to readily proceed within the LC matrix, just by irradiating the two-component LC. Compared with traditional LC media, such a system seems to have obvious advantages in the following aspects; (1) the relative orientation

**Scheme 1.** Schematic Representation of the Photoreaction within Liquid Crystalline Media



of the substrate (carboxylic acid) molecules is considered to be well-defined because the substrate itself is the component of the LC, (2) every photoreactive molecule intimately interacts with a chiral source amino alcohol by hydrogen-bonding interaction and salt-pair formation, and (3) owing to the availability of various photoreactive carboxylic acids, as well as the noncovalency of interaction between the two components, such amino alcohol units would offer special environments to various substrates/reactions.

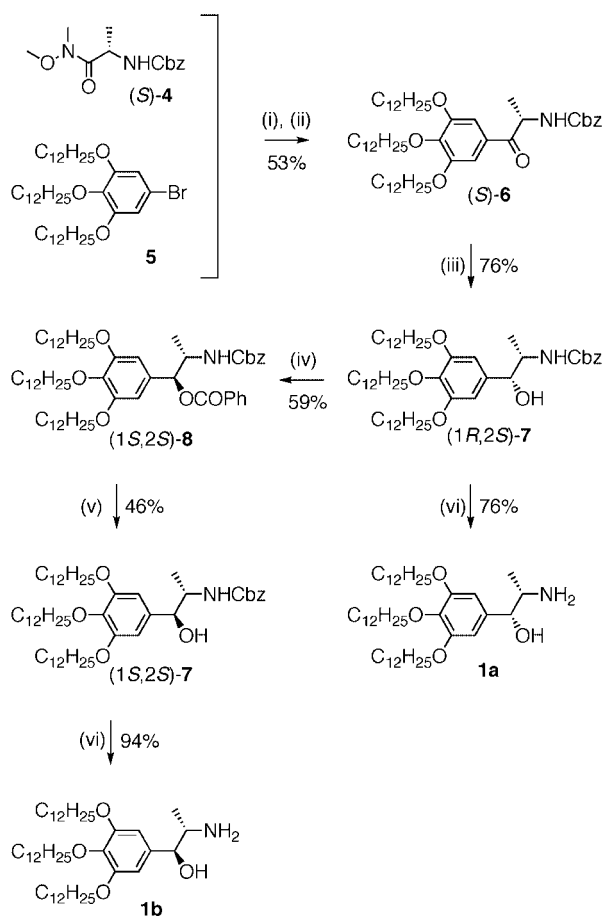
For such a conceptually new approach, we have recently reported preliminary results on the application of a two-component LC as a reaction medium (Scheme 1), in which the photodimerization of 2-anthracenecarboxylic acids proceeded in satisfactory yield with unprecedented high enantioselectivity.<sup>13</sup> In order to expand the scope of this methodology, variation of the amphiphilic amino alcohol unit, having been limited to only one example up to now, should be increased. For the initial stage of our ongoing study, we focused on the variation in stereochemistry of the amino alcohol unit. Here we report, in detail, the design, synthesis, and reaction-controlling ability of three amphiphilic amino alcohols (**1a–c**), the sizes and shapes of which are similar, but the stereochemistries of the stereogenic carbons adjacent to the amino (C2) and hydroxy (C1) groups are systematically varied (the stereochemistry of C1/C2: **1a** *R/S*, **1b** *S/S*, and **1c** *S*/achiral).

## 2. Results and Discussion

**2.1. Design of the Amphiphilic Amino Alcohols 1a–c.** We have recently found that the salt of (–)-norephedrine with an achiral amphiphilic carboxylic acid exhibited a very stable LC phase.<sup>12</sup> On the basis of the result, in the present study we at first designed the chiral amphiphilic amino alcohol **1a** with an

- (5) (a) Lehn, J.-M. *Science* **1985**, *227*, 849–856. (b) Conn, M. M.; Rebek, J. *Chem. Rev.* **1997**, *97*, 1647–1668. (c) Rebek, J. *Angew. Chem., Int. Ed.* **2005**, *44*, 2068–2078. (d) Yoshizawa, M.; Fujita, M. *Pure Appl. Chem.* **2005**, *77*, 1107–1112.
- (6) (a) Muthuramu, K.; Ramamurthy, V. *J. Org. Chem.* **1982**, *47*, 3976–3979. (b) Wolff, T.; Müller, N.; von Büna, G. *J. Photochem.* **1983**, *22*, 61–70. (c) Lv, F.-F.; Chen, B.; Wu, L.-Z.; Zhang, L.-P.; Tung, C.-H. *Org. Lett.* **2008**, *10*, 3473–3476.
- (7) (a) Lin, Y. C.; Weiss, R. G. *Macromolecules* **1987**, *20*, 414–417. (b) Bhat, S.; Maitra, U. *Molecules* **2007**, *12*, 2181–2189. (c) Dawn, A.; Fijita, N.; Haraguchi, S.; Sato, H.; Sada, K.; Shinkai, S. *Chem. Commun.* **2009**, 2100–2102.
- (8) (a) Imae, T.; Tsubota, T.; Okamura, H.; Mori, O.; Takagi, K.; Itoh, M.; Sawaki, Y. *J. Phys. Chem.* **1995**, *99*, 6046–6053. (b) Li, H. R.; Wu, L. Z.; Tung, C. H. *J. Am. Chem. Soc.* **2000**, *122*, 2446–2451.
- (9) For examples of organic transformations in liquid crystalline reaction media, see the following reviews and references cited therein: (a) Weiss, R. G. In *Photochemistry in Organized and Constrained Media*; Ramamurthy, V., Ed.; VCH: New York, 1991, Chapter 14. (b) Leigh, W. J.; Workentin, M. S. In *Liquid Crystals as Solvents for Spectroscopic, Chemical Reaction, and Gas Chromatographic Applications; Handbook of Liquid Crystals*; Demun, D., Ed. Wiley-VCH: Weinheim, 1998; pp 839–895.
- (10) (a) Saeva, F. D.; Sharpe, P. E.; Oline, G. R. *J. Am. Chem. Soc.* **1975**, *97*, 204–205. (b) Verbit, L.; Halbert, T. R.; Patterson, R. B. *J. Org. Chem.* **1975**, *40*, 1649–1650. (c) Pirkle, W. H.; Rinaldi, P. L. *J. Am. Chem. Soc.* **1977**, *99*, 3510–3511. (d) Eskenazi, C.; Nicoud, J. F.; Kagan, H. B. *J. Org. Chem.* **1979**, *44*, 995–999.
- (11) For selected examples of recent attempts to apply LC media to the fabrication of meso-scaled supramolecular architectures, see: (a) Akagi, K.; Piao, G.; Kaneko, S.; Sakamaki, K.; Shirakawa, H.; Kyotani, M. *Science* **1998**, *282*, 1683–1686. (b) Kitamura, T.; Nakaso, S.; Mizoshita, N.; Tochigi, Y.; Shimomura, T.; Moriyama, M.; Ito, K.; Kato, T. *J. Am. Chem. Soc.* **2005**, *127*, 14769–14775. (c) Dobbs, W.; Suisse, J.-M.; Douce, L.; Welter, R. *Angew. Chem., Int. Ed.* **2006**, *45*, 4179–4182.
- (12) (a) Ishida, Y.; Amano, S.; Saigo, K. *Chem. Commun.* **2003**, 2338–2339. (b) Ishida, Y.; Amano, S.; Iwahashi, N.; Saigo, K. *J. Am. Chem. Soc.* **2006**, *128*, 13068–13069. (c) Amano, S.; Ishida, Y. K.; Saigo, K. *Chem.—Eur. J.* **2007**, *13*, 5186–5196.

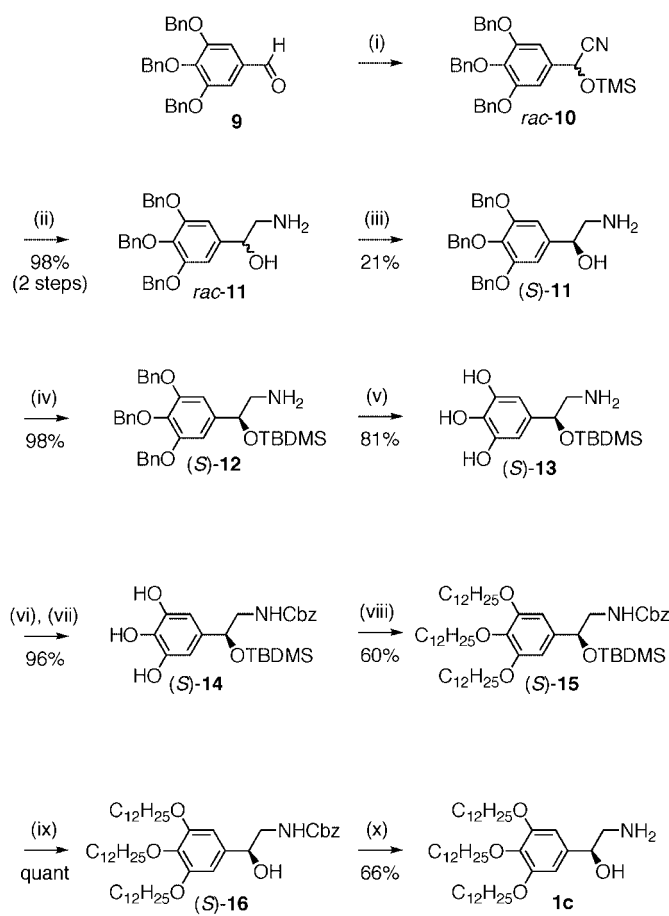
- (13) Ishida, Y.; Kai, Y.; Kato, S.; Misawa, A.; Amano, S.; Matsuoka, Y.; Saigo, K. *Angew. Chem., Int. Ed.* **2008**, *47*, 8241–8245.

Scheme 2. Stereocontrolled Synthesis of the Amphiphilic Amino Alcohols **1a–c**(a) Synthesis of **1a** and **1b**

(i) (**S**)-**4**, *n*BuLi (1.0 eq), THF,  $-78^{\circ}\text{C}$  to rt, 30 min; (ii) **5**, *n*BuLi (1.0 eq),  $\text{Et}_2\text{O}$ , rt, 2 h, then the mixture of step i,  $-20^{\circ}\text{C}$ , 3 h; (iii)  $\text{Al}(\text{O}i\text{Pr})_3$  (0.3 eq), *i*PrOH/ $\text{CH}_3\text{Ph}$ ,  $50^{\circ}\text{C}$ , 48 h; (iv)  $\text{PhCO}_2\text{H}$  (2.0 eq),  $\text{PPh}_3$  (1.5 eq), *i*PrOCON= $\text{NCO}_2i\text{Pr}$  (1.5 eq),  $\text{CH}_3\text{Ph}$ , rt, 2 h; (v)  $\text{LiAlH}_4$  (4.0 eq), THF,  $0^{\circ}\text{C}$ , 2 h; (vi)  $\text{H}_2$  (1 atm), Pd/C (cat.), EtOH, rt, 12 h.

absolute configuration of (1*R*,2*S*), which is similar to that of (–)-norephedrine. On the other hand, it is well-known that diastereomers often show chirality-induction abilities quite different from each other. Therefore, the epimeric amino alcohol of **1a**, the amino alcohol **1b** with an absolute configuration of (1*S*,2*S*), was designed. Moreover, in order to clarify the role of chirality at the C1 and C2 positions in **1a/1b**, the synthesis of a simpler analogue, **1c**, was also tried. Since **1c** lacks a methyl group at the C2 position, it has only one stereogenic carbon at the C1 position.

**2.2. Stereocontrolled Synthesis of the Amphiphilic Amino Alcohols 1a–c.** The two amino alcohols bearing a C2-methyl group, **1a** and **1b**, were synthesized as follows: An aryllithium, prepared by treating the bromobenzene derivative **5**<sup>14</sup> with butyllithium, was coupled with the alanine derivative (**S**)-**4**<sup>15</sup> to form (**S**)-**6**,<sup>16</sup> which was then reduced by applying the Meerwein–Ponndorf–Verley method; the reduction proceeded

(b) Synthesis of **1c**

(i)  $\text{Me}_3\text{SiCN}$  (1.1 eq), ZnI (cat.),  $\text{CH}_2\text{Cl}_2$ , rt, 5 h; (ii)  $\text{LiAlH}_4$  (2.5 eq),  $\text{Et}_2\text{O}$ , reflux, 3 h; (iii) (**S**)-mandelic acid, recrystallization from EtOH (x 3) and from EtOH/MeOH (x 2); (iv) *t*BuMe<sub>2</sub>SiCl (1.1 eq), imidazole (2.0 eq), DMAP (0.1 eq),  $\text{CH}_2\text{Cl}_2$ , rt, 24 h; (v)  $\text{H}_2$  (1 atm), Pd/C (cat.), EtOH, rt, 24 h; (vi)  $\text{Me}_3\text{SiCl}$  (3.0 eq), pyridine, rt, 90 min; (vii)  $\text{CbzCl}$  (2.0 eq), pyridine, rt, 4 h; (viii)  $\text{C}_{12}\text{H}_{25}\text{Br}$  (4.2 eq),  $\text{K}_2\text{CO}_3$  (15 eq), DMF,  $90^{\circ}\text{C}$ , 6 h; (ix)  $\text{Bu}_4\text{N}\cdot\text{F}$  (10 eq), AcOH (10 eq), rt, 24 h; (x)  $\text{H}_2$  (1 atm), Pd/C (cat.), ethanol, rt, 24 h.

with excellent diastereoselectivity in an *anti*-Cram manner to afford the (1*R*,2*S*)-isomer ((1*R*,2*S*)-**7**) in a stereopure form.<sup>17</sup> By the simple hydrogenolysis of the N-protecting group in (1*R*,2*S*)-**7**, one of the target molecules (**1a**) was successfully obtained (Scheme 2a, right). Its epimer, **1b**, was also synthesized from the same precursor (1*R*,2*S*)-**7** via the Mitsunobu inversion at the C1 position forming the corresponding ester (1*S*,2*S*)-**8**,<sup>18</sup> followed by the successive cleavages of the O- and N-protecting groups (Scheme 2a, left).

(14) Wu, J.; Watson, M. D.; Zhang, L.; Wang, Z.; Müllen, K. *J. Am. Chem. Soc.* **2004**, *126*, 177–186.

(15) Kano, S.; Yokomatsu, T.; Iwasawa, H.; Shibuya, S. *Tetrahedron Lett.* **1987**, *28*, 6331–6334.

(16) Davies, D. T.; O'hanlon, P. J. *Synth. Commun.* **1988**, *18*, 2273–2280.

(17) Yin, J.; Huffman, M. A.; Conrad, K. M.; Armstrong, J. D., III *J. Org. Chem.* **2006**, *71*, 840–843.

(18) Mitsunobu, O. *Synthesis* **1981**, 1–28.



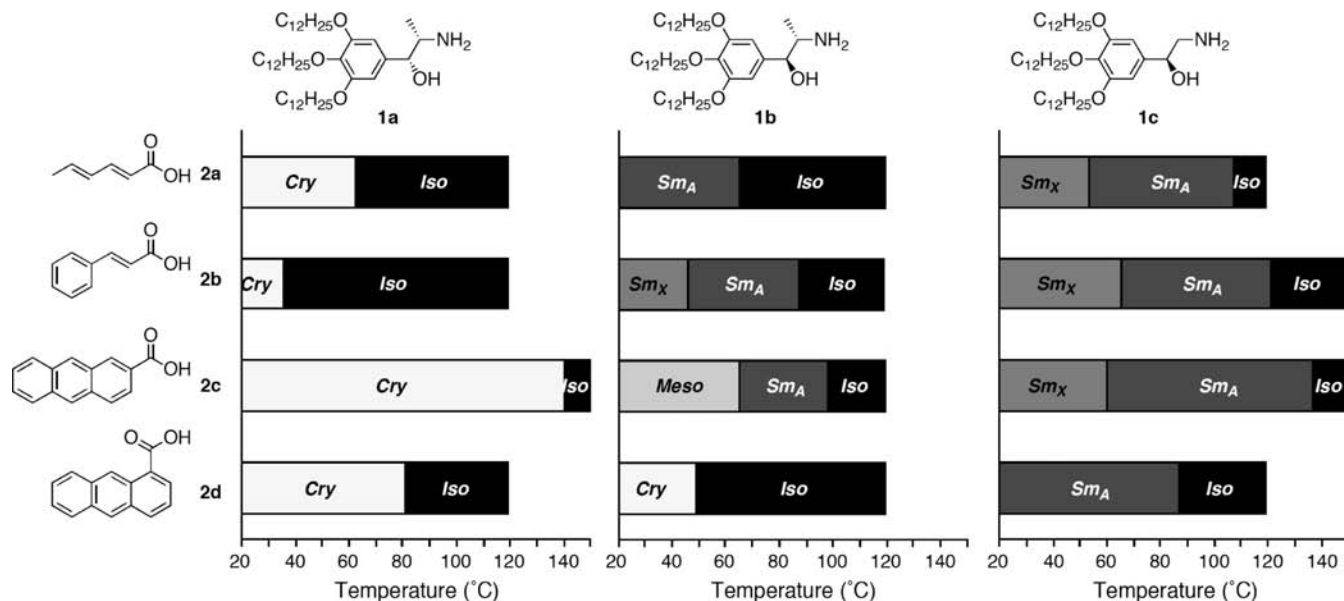


**Figure 1.** Thermotropic behavior of the salts of amphiphilic amino alcohols (**1a–c**) with photoreactive carboxylic acids (**2a–d**) in a cooling process. Iso = isotropic phase, Sm<sub>A</sub> = smectic A phase, Sm<sub>X</sub> = smectic phase other than Sm<sub>A</sub>, Meso = unidentified mesophase, Cry = crystalline phase.

One of the most beneficial features of the present synthetic route is potential applicability to the synthesis of other amphiphilic amino alcohols; not only the alanine derivative (*S*)-**4**, various enantiopure amino-acid derivatives are available as the starting material, which would provide stereoregulated, amphiphilic amino alcohols bearing the corresponding substituent at the C2 position.

In the syntheses of **1a** and **1b**, one of the two stereogenic carbons (C2) was originated from the starting amino acid, while the stereochemistry of the other (C1) was controlled by the neighboring effect of the stereoregulated C2. Contrary to them, **1c** has only one stereogenic carbon at the C1 position, meaning that the same strategy is not applicable to the synthesis of **1c**. Thus, a new synthetic method was developed, which involves the enantioseparation (Scheme 2b). The aldehyde **9**<sup>19</sup> was converted into a racemic 2-amino alcohol (*rac*-**11**) via a well-established series of reactions, the cyanohydrin formation followed by the hydride reduction of the nitrile group.<sup>20</sup> Fortunately, the enantiomers of **11** could be easily separated by the diastereomer salt method by using mandelic acid as the most suitable resolving agent. Owing to the convenience and scalability of this method, both enantiomers of **11** were obtained in a gram scale. The absolute configuration of **11** was deduced from the configuration of (*S*)-mandelic acid already known; we succeeded in obtaining the X-ray crystal structure of the salt of (*R*)-**11** with (*S*)-mandelic acid. The enantiopure (*S*)-**11** thus obtained was then derived into the target amphiphilic 2-amino alcohol **1c** through the protection of the hydroxy group, the hydrogenolysis of the benzyl ether moieties, the protection of the amino group, the coupling of the phenolic hydroxy groups with dodecyl bromide, and the deprotection of the hydroxy and amino groups.

**2.3. Thermotropic Behavior of the Salts of Amphiphilic Amino Alcohols (1a–c) with Photo-Reactive Carboxylic Acids (2a–d).** With the three types of amphiphilic amino alcohols (**1a–c**) in hand, we next prepared and characterized their salts with four kinds of photoreactive carboxylic acids, sorbic acid (**2a**), cinnamic acid (**2b**), 2-anthracenecarboxylic acid

(**2c**), and 1-anthracenecarboxylic acid (**2d**). Typically, equimolar amounts of the amino alcohol and the carboxylic acid were dissolved in 2-propanol, and the solvent was removed to dryness to give the corresponding salt as a solid or waxy oil. For every combination of the acids and bases employed here, the formation of ammonium-carboxylate salt pair was unambiguously confirmed by IR spectroscopy; an absorption attributable to the C=O vibration was observed at 1620–1650 cm<sup>-1</sup>, which was notably shifted from the corresponding absorption of usual free carboxylic acids (1680–1695 cm<sup>-1</sup>).

The thermotropic behavior of these amphiphilic salts was investigated by using a combination of differential scanning calorimetry (DSC), polarized optical microscopy (POM), and X-ray diffraction analysis (XRD). Through a cooling process from an isotropic melt, transitions into crystalline and/or LC phase(s) were clearly monitored by POM, where characteristic textures were generated. Transition temperatures and their enthalpy changes were obtained by DSC operated at a scanning rate of 5 °C min<sup>-1</sup>.

Upon repeating heating and cooling cycles, essentially identical DSC traces were observed in good reproducibility, except for the first heating. These observations strongly suggest that undesired thermal events, such as the decomposition of the components and the cleavage of the salt pair, did not take place within the thermal range of the DSC measurement (–50 to 160 °C), which was confirmed by <sup>1</sup>H NMR and IR spectroscopy. On a heating process, some salts showed complicated thermotropic behaviors involving crystal-to-crystal phase transition(s), of which the DSC peaks were overlapped with each other. Judging from the DSC traces of the first/second heating and cooling processes, some mesophases appeared in the cooling processes were monotropic (Figure 1, Sm<sub>A</sub>[**1b**·**2a**], Sm<sub>X</sub>[**1b**·**2b**], Sm<sub>A</sub>[**1b**·**2c**], Meso[**1b**·**2c**], and Sm<sub>X</sub>[**1c**·**2c**], and Sm<sub>A</sub>[**1c**·**2d**]). Although such metastable phases may turn into other phases, which is not favorable as reaction media, their lifetime was confirmed to be long enough (1–20 h) for the

(19) Zaveri, N. T. *Org. Lett.* **2001**, *3*, 843–846.

(20) Kirk, K. L.; Cantacuzene, D.; Collins, B.; Chen, G. T.; Nimit, Y.; Creveling, C. R. *J. Med. Chem.* **1982**, *25*, 680–6844.

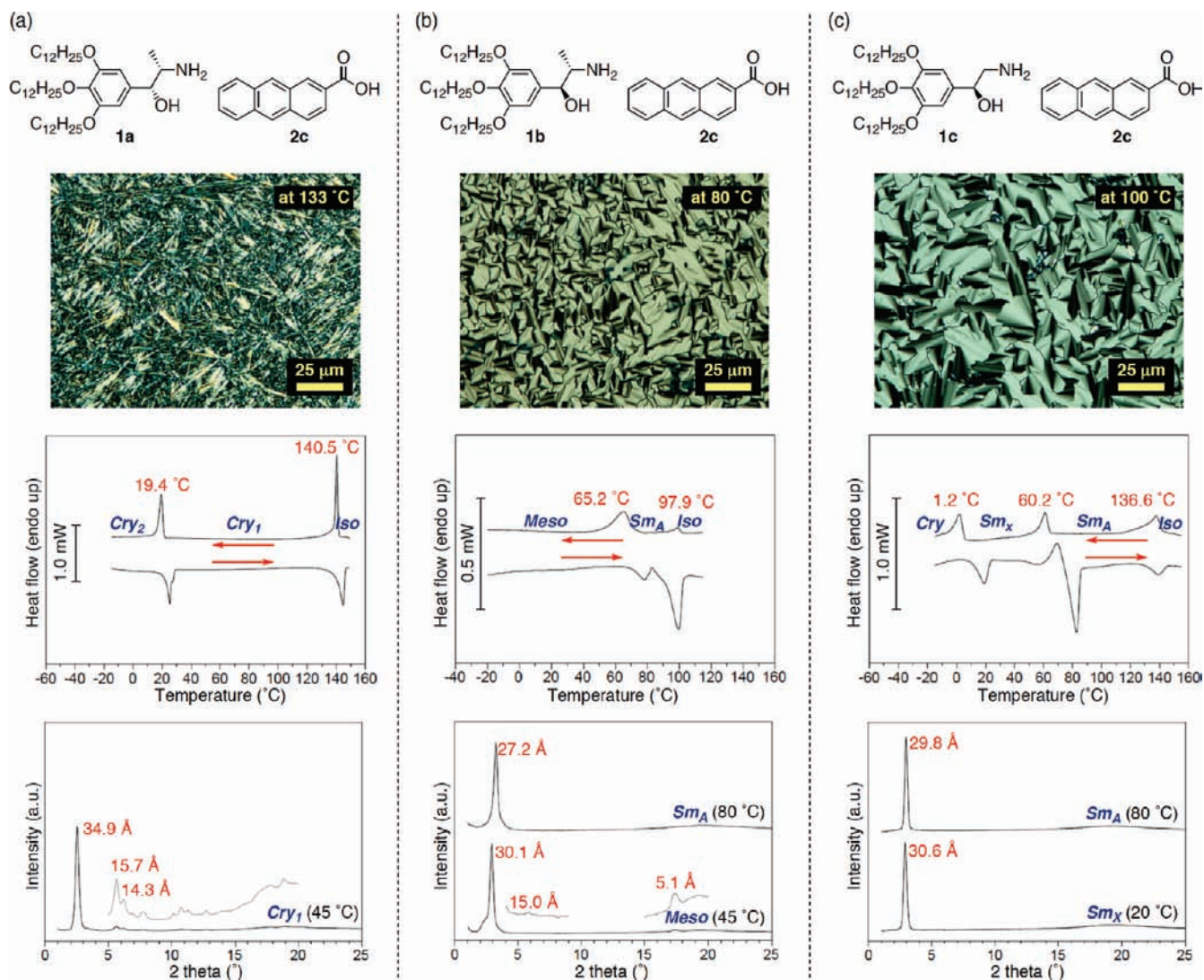


**Figure 2.** Polarized optical microscopy images (top), differential scanning calorimetry traces (middle), and X-ray diffraction profiles (bottom) of the amphiphilic salts (a) **1a**·**2c**, (b) **1b**·**2c**, and (c) **1c**·**2c**.

present photoreactions. In addition, these LC phases appeared in good reproducibility when the system was cooled slower ( $-2.5\text{ °C min}^{-1}$ ). Therefore, we focused only on a cooling process from an isotropic melt to simplify the comparison of the thermotropic behavior of the salts. The lattice patterns of these phases were estimated by XRD measurements. The phase transition behavior of the twelve salts is summarized in Figure 1.

Contrary to our expectation based on the thermotropic behavior of the salt of an amphiphilic carboxylic acid with (–)-norephedrine,<sup>12</sup> none of the salts derived from **1a**, which has an absolute configuration similar to that of (–)-norephedrine, exhibited LC phase; a direct transition from an isotropic phase to a crystalline phase was commonly observed. In sharp contrast, **1b** and **1c** showed high propensity to form LC salts with wide thermal ranges; seven of the eight salts (**1b**·**2a–c** and **1c**·**2a–d**) exhibited one or two LC phase(s). Most of the mesophases showed an XRD pattern characteristic to a smectic lattice with a strong fundamental (001) reflection at  $\sim 30\text{ Å}$ , accompanied with a diffusive reflection around  $4.5\text{ Å}$  (Figure 2, bottom). In POM observation, some of these smectic LCs exhibited a focal conical texture, strongly indicative of smectic A ( $Sm_A$ ) phase (Figure 2b and Figure 2c, top). Among the mesophases found

here,  $Meso[1b\cdot 2c]$  was an exception. Apparently, its XRD pattern seems to be a smectic phase with higher order than  $Sm_A$ , characterized with sharp reflections at  $30\text{ Å}$  [(001)],  $15\text{ Å}$  [(002)], and  $5\text{ Å}$  [most likely (100)], as well as a diffusive reflection around  $4.5\text{ Å}$ . However, the (001) reflection was overlapped with an unknown broad reflection (Figure 2b, bottom). Considering the hydrophobic–hydrophilic volume ratio of these amphiphilic salts, these salts were expected to take a bilayer-like structure, which might lead to the formation of smectic or related structures. The observed  $d$ -spacings were shorter than anticipated from extended molecular modeling, most likely due to the partial interdigitation of the aliphatic tails (Figure 3).<sup>21</sup>

As summarized in Figure 1, a subtle change in the structure of the amino alcohol unit, regarding the substituent at and the stereochemistry of the C2 position, brought a significant effect

(21) Such a difference between the observed and anticipated  $d$ -spacings can be elucidated not only by the interdigitation of the alkyl chains but also by the tilting of the bilayers. The latter case should lead to the formation of a  $Sm_C$  structure. In POM observations, however, most of the LC salts exhibited a typical focal conical texture often observed for  $Sm_A$  phases, while the textures characteristic of smectic C phases, such as broken focal conic and Schlieren textures, were not observed.



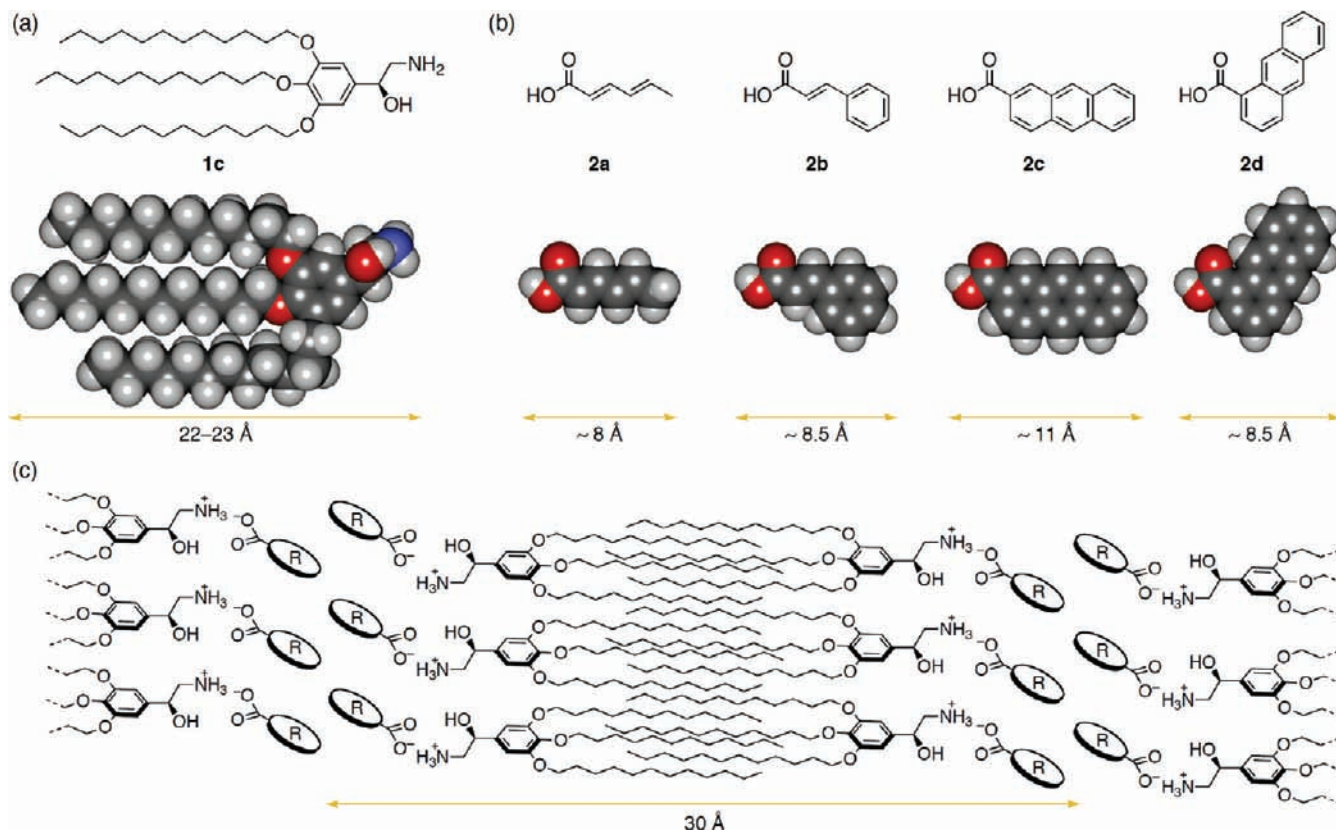


**Figure 3.** Schematic representation of the structures of (a) the amphiphilic amino alcohol **1c**, (b) the photoreactive carboxylic acids **2a–d**, and (c) the self-assembled bilayer.

on the thermotropic behavior of their salts, although the substituent at this position contributes less than 2% of the total molecular weight of an amphiphilic salt.<sup>22</sup> This observation might reveal the risk of our preconception that the self-organization of amphiphilic molecules can be simply elucidated on the basis of a hydrophilic–hydrophobic volume ratio. Among these three amino alcohols, **1c** had the strongest propensity to form LC salts with a wide thermal window; all of the four salts derived from **1c** exhibited one or two kinds of LC phase(s). Moreover, in the case of **1b**, three of the four salts showed LC phase(s), and their clearing temperatures were generally lower than those of the corresponding salts composed of **1c**. In sharp contrast, all of the salts derived from **1a** exhibited no LC phase; a direct transition from an isotropic phase to a crystalline phase was commonly observed.

To elucidate the effect of the state of the salts (isotropic, LC, or crystalline) on an in situ reaction (efficiency and selectivity), the salts of **1a**, which showed exceptionally high crystallinity, would provide some insights. At an appropriate temperature, the salts of **1b** and/or **1c** exhibit LC phases, while the corresponding salt of **1a** exists as a crystal. Therefore, photoreactions can be conducted at the same temperature in these crystalline and LC states, which would enable us to directly compare the results of the photoreactions, free from the effect of the reaction temperature.

**2.4. General Aspects of the Photodimerization of Anthracenecarboxylic Acids.** In the next stage, we conducted the photoinduced transformation of carboxylic acid units within

the amphiphilic salt matrices. Our strategy is principally applicable to the reactions of all carboxylic acids (**2a–d**), which is undoubtedly the ultimate goal of our ongoing study. However, at first we planned to carry out the photodimerization of anthracene derivatives (**2c**, 2-anthracenecarboxylic acid; **2d**, 1-anthracenecarboxylic acid), because its simplicity seemed to be advantageous to clarify the effect of the stereochemistry of the amino alcohol units. The photodimerization of anthracene derivatives is a well-established, simple [4 + 4] cycloaddition, which hardly involves complicated side reactions such as the isomerization of the monomeric unit.<sup>23</sup> In addition, it still remains as a challenge to control the regio- and stereochemistries of the photodimerization of laterally substituted anthracene derivatives; the photodimerization of dissymmetric anthracene derivatives like **2c** and **2d** principally gives rise to no less than four configurational isomers (*head-to-head/head-to-tail* isomers with *syn/anti* isomerism, denoted as *syn*<sup>HH</sup>, *anti*<sup>HH</sup>, *syn*<sup>HT</sup>, and *anti*<sup>HT</sup>), two isomers of which consist of a pair of C<sub>2</sub>-enantiomers, respectively ((*R*)/(*S*)-*anti*<sup>HH</sup> and (*R*)/(*S*)-*syn*<sup>HT</sup>).

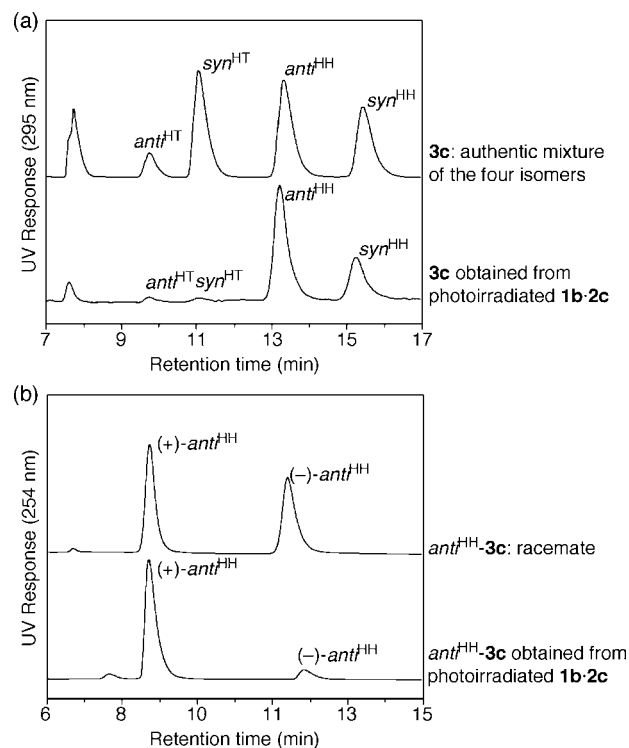
To date, the environment-directed photodimerization of 2-anthracenecarboxylic acid (**2c**) have been extensively studied, by using various hosts including cyclodextrins, modified cyclodextrins, proteins, amine receptors, and organogel matrices.<sup>24–26</sup> Owing to a wealth of data having been reported on regio-/diastereo-/enantiocontrols, the photodimerization of **2c** has become a ‘benchmark’ reaction to evaluate the ability of

(22) Percec, V.; Dulcey, A. E.; Peterca, M.; Adelman, P.; Samant, R.; Balagurusamy, V. S. K.; Heiney, P. A. *J. Am. Chem. Soc.* **2007**, *129*, 5992–6002.

(23) For general aspects of the photodimerization of anthracenes, see: (a) Bouas-Laurent, H.; Desvergne, J.-P.; Castellan, A.; Lapouyade, R. *Chem. Soc. Rev.* **2000**, *29*, 43–55. (b) Bouas-Laurent, H.; Desvergne, J.-P.; Castellan, A.; Lapouyade, R. *Chem. Soc. Rev.* **2001**, *30*, 248–263.

supramolecular systems to derive a controlled reaction. Nevertheless, successful examples have been surprisingly limited, especially in terms of enantiocontrol. In a recent noticeable achievement, Inoue and co-workers have reported a highly enantioselective photodimerization of **2c** within hydrophobic cavities of human serum albumin to afford the *syn*<sup>HT</sup>- and *anti*<sup>HH</sup>-dimers with excellent enantiomeric excesses (up to 82 and 90% ee, respectively). Unfortunately, the net overall yields of these isomers were at an unsatisfactory level (5.9 and 1.0% net overall yield, respectively) due to the problems in regio-/diastereoselectivities and conversion.<sup>24e</sup> More recently, the same research group has succeeded in the highly regio-/diastereo-/enantioselective formation of the *syn*<sup>HT</sup>-dimer in excellent yield (up to 91% ee, >65% net overall yield); in this work, a derivative of **2c** covalently modified with  $\alpha$ -cyclodextrin was used as a substrate, while  $\gamma$ -cyclodextrin was used as a host molecule.<sup>25c</sup> On the other hand, the photodimerization of **2d** has not been extensively investigated thus far. However, the reaction should be another attractive target, considering its simple reaction course and complicated regio-/stereochemistries, are similar to those of **2c**.<sup>27</sup>

**2.5. Photodimerization of 2-Anthracenecarboxylic Acid (2c) in the Amphiphilic Salts.** The in situ photodimerization of 2-anthracenecarboxylic acid (**2c**) was conducted by irradiating the salt (**1a**·**2c**, **1b**·**2c**, or **1c**·**2c**) with UV/vis light (500 W, a high-pressure mercury arc lamp, >380 nm) under argon atmosphere. The photoirradiated sample was then treated with an excess amount of trimethylsilyldiazomethane to esterify the carboxyl groups in the system, and volatiles were removed under reduced pressure. The resultant mixture was applied to <sup>1</sup>H NMR spectroscopy (CDCl<sub>3</sub>) to estimate the yield of the photodimerization. From the mixture, the esterified photodimers were isolated by preparative silica gel TLC, and the isomer distribution was evaluated by a two-stage normal-phase HPLC analysis (Figure 4).<sup>28</sup> Because the methylation proceeded quantitatively, the yield and isomer distribution of the photodimer diesters **3c** should be essentially identical to those of the original photodimers. The results are summarized in Table 1.

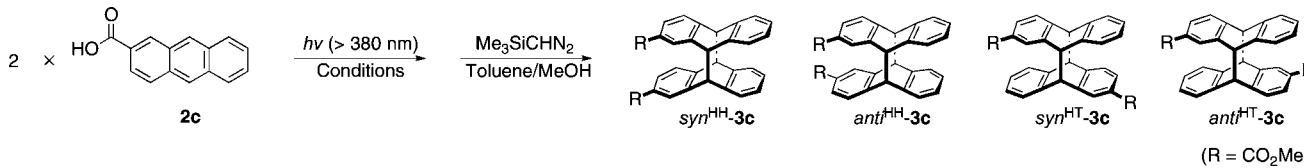


**Figure 4.** (a) Estimation of the isomer distribution by achiral HPLC. An authentic mixture of the four isomers of **3c** (top) and a mixture obtained from photoirradiated **1b**·**2c** (bottom). (b) Estimation of the enantiomeric ratio of *anti*<sup>HH</sup>-**3c** by chiral HPLC. An authentic racemate of *anti*<sup>HH</sup>-**3c** (top) and *anti*<sup>HH</sup>-**3c** obtained from photoirradiated **1b**·**2c** (bottom).

**2.5.1. Reactivity.** In all phases of the amphiphilic salts, the photodimerization underwent cleanly to afford a mixture of the photodimers, where only the formation of 2-anthraquinonecarboxylic acid was a detectable side reaction (<1%). When the photodimerization was conducted in the isotropic phases, excellent yields were realized after 1-h irradiation, without depending on the amino alcohol unit (entries 3, 11, and 16, Iso[**1a**·**2c**], Iso[**1b**·**2c**], and Iso[**1c**·**2c**], 83–91% yield). As was expected, the LC phases also showed acceptable to good reactivity (entries 4–8, Meso[**1b**·**2c**]; entries 9 and 10, Sm<sub>A</sub>[**1b**·**2c**]; entries 12 and 13, Sm<sub>X</sub>[**1c**·**2c**]; entries 14 and 15, Sm<sub>A</sub>[**1c**·**2c**]). Although the reaction rate in the LC phases was lower than that in the isotropic phases, all of the LC reaction systems attained satisfactory yields after enough irradiation (entries 5, 8, 9, 13 and 15, 58–85% yield). Among them, the two LC phases of **1c**·**2c** realized yields almost comparable to those in the isotropic phases (entry 13, Sm<sub>X</sub>[**1c**·**2c**], 85% yield; entry 15, Sm<sub>A</sub>[**1c**·**2c**], 81% yield). Contrary to **1c**·**2c**, the crystalline phase of **1a**·**2c** (Cry[**1a**·**2c**]) afforded a mixture of the photodimers in unsatisfactory yield, even after adequate irradiation at higher temperatures (entries 1 and 2, Cry[**1a**·**2c**],

- (24) For selected examples of the photodimerization of 2-anthracenecarboxylic acid, see: (a) Tamaki, T.; Kokubu, T.; Ichimura, K. *Tetrahedron* **1987**, *43*, 1485–1494. (b) Ito, Y.; Olovsson, G. *J. Chem. Soc., Perkin Trans. 1* **1997**, 127–133. (c) Nakamura, A.; Inoue, Y. *J. Am. Chem. Soc.* **2003**, *125*, 966–972. (d) Ikeda, H.; Nihei, T.; Ueno, A. *J. Org. Chem.* **2005**, *70*, 1237–1242. (e) Nishijima, M.; Wada, T.; Mori, T.; Pace, T. C. S.; Bohne, C.; Inoue, Y. *J. Am. Chem. Soc.* **2007**, *129*, 3478–3479. (f) Reference 7c. (g) Reference 12. (h) Kawanami, Y.; Pace, T. C. S.; Mizoguchi, J.; Yanagi, T.; Nishijima, M.; Mori, T.; Wada, T.; Bohne, C.; Inoue, Y. *J. Org. Chem.* **2009**, *74*, 7908–7921. (i) Ke, C.; Yang, C.; Mori, T.; Wada, T.; Liu, Y.; Inoue, Y. *Angew. Chem., Int. Ed.* **2009**, *48*, 6675–6677.
- (25) For the photodimerization of 2-anthracenecarboxylic acid esters/amides, see: (a) de Schryver, F. C.; de Brackeleire, M.; Toppet, S.; van Schoor, M. *Tetrahedron Lett.* **1973**, *15*, 1253–1256. (b) Hiraga, H.; Morozumi, T.; Nakamura, H. *Eur. J. Org. Chem.* **2004**, 4680–4687. (c) Yang, C.; Mori, T.; Origane, Y.; Ko, Y. H.; Selvapalam, N.; Kim, K.; Inoue, Y. *J. Am. Chem. Soc.* **2008**, *130*, 8574–8575. (d) Dawn, A.; Shiraki, T.; Haraguchi, S.; Sato, H.; Sada, K.; Shinkai, S. *Chem.—Eur. J.* **2010**, *16*, 3676–3689.
- (26) For the photodimerization of anthracenes in liquid crystals, see: (a) Méry, S.; Haristoy, D.; Nicoud, J.-F.; Guillon, D.; Monobe, H.; Shimizu, Y. *J. Mater. Chem.* **2003**, *13*, 1622–1630. (b) Takaguchi, Y.; Tajima, T.; Yanagimoto, Y.; Tsuboi, S.; Ohta, K.; Motoyoshiya, J.; Aoyama, H. *Org. Lett.* **2003**, *5*, 1677–1679.
- (27) For the photodimerization of 1-anthracenecarboxylic acid and its esters/amides, see: (a) Reference 24a. (b) Ueno, A.; Moriwaki, F.; Iwama, Y.; Suzuki, I.; Osa, T.; Ohta, T.; Nozoe, S. *J. Am. Chem. Soc.* **1991**, *113*, 7034–7036. (c) Becker, H.-D.; Becker, H.-C.; Langer, V. *J. Photochem. Photobiol. A* **1996**, *97*, 25–32. (d) Reference 24b.

- (28) As an established method to estimate the isomer distribution of the photodimer of **2c**, an HPLC analysis based on tandem reversed-phase columns (Inertsil ODS-2 and Chiralcel OJ-R) has been widely used (ref 24c). However, this method does not seem to be optimal for the reaction systems containing hydrophobic components; for HPLC injection, samples should be pre-treated to remove the hydrophobic component, which has a risk of biasing the distribution of isomers. In addition, due to the inherent hydrophobicity of the photodimer of **2c**, retention times of the isomers were relatively long, which is problematic for the accurate estimation of the peak area. Therefore, we developed an alternative method, based on the esterification of carboxyl groups in the system, followed by two-stage normal-phase HPLC (see Supporting Information).

**Table 1.** Photodimerization of 2-Anthracenecarboxylic Acid (**2c**)<sup>a</sup>


entry	medium	phase	temp. (°C)	time (h)	yield (%) <sup>d</sup>	product ratio (%) <sup>e</sup>				ee (%) <sup>f</sup> anti <sup>HH</sup>
						syn <sup>HH</sup>	anti <sup>HH</sup>	syn <sup>HT</sup>	anti <sup>HT</sup>	
1	<b>1a</b>	Cry	40	15	10	57	41	1	1	-15
2		Cry	80	15	23	52	44	2	2	-16
3		Iso	160	1	89	50	36	4	10	-14
4	<b>1b</b>	Meso	35	3	23	26	72	1	1	+78
5		Meso	35	15	58	27	71	1	1	+74
6		Meso	45	1	24	27	71	1	1	+86
7		Meso	45	3	48	28	70	1	1	+81
8		Meso	45	15	68	34	64	1	1	+67
9		Sm <sub>A</sub>	80	1	72	46	52	1	1	+45
10		Sm <sub>A</sub>	80	3	66	48	49	2	1	+26
11		Iso	110	1	83	52	45	2	1	+18
12	<b>1c</b>	Sm <sub>X</sub>	40	3	42	56	42	1	1	+31
13		Sm <sub>X</sub>	40	15	85	56	43	1	1	+32
14		Sm <sub>A</sub>	105	1	64	61	37	1	1	+14
15		Sm <sub>A</sub>	105	3	81	61	37	1	1	+16
16		Iso	160	1	91	56	41	2	1	+13
<sup>b</sup>	H <sub>2</sub> O	Sol	25	1	88	7	14	36	43	n.d.
<sup>c</sup>	CH <sub>2</sub> Cl <sub>2</sub>	Sol	25	2	96	21	7	22	32	n.d.

<sup>a</sup> Irradiated at  $\lambda = >380$  nm under argon. <sup>b</sup> Irradiated at  $\lambda = >320$  nm under argon in a phosphate buffer solution (pH 7.0). See ref 24e. <sup>c</sup> Irradiated at  $\lambda = >320$  nm under argon in dichloromethane. See ref 24h. <sup>d</sup> Determined by <sup>1</sup>H NMR. <sup>e</sup> Isomer distribution of **3c** estimated by achiral HPLC. <sup>f</sup> Enantiomeric excess of anti<sup>HH</sup>-**3c** estimated by chiral HPLC. The signs + and - represent that the major product was the first- and second-eluted enantiomer in the chiral HPLC analysis, respectively.

10 and 23% yield). Taking account of the reaction temperatures employed here, such a large difference in reaction efficiency between the LC and crystalline phases is not attributable to the difference in reaction temperature, but to the difference in molecular mobility.

**2.5.2. HH/HT Selectivity.** Regardless of the choice of the amino alcohol unit or phase, almost all of the present reaction systems showed surprisingly high HH/HT selectivities (HH:HT = 97:3–98:2). The only exception was the isotropic phase of **1a**·**2c** (entry 3, Iso[**1a**·**2c**], HH:HT = 86:14); even in this case, the HH/HT selectivity was still superior to those of most of conventional supramolecular reaction systems designed for the control of this reaction. As far as we are aware of, the HH/HT ratios achieved here are at the highest level in the photodimerization of **2c**. In the absence of environmental constraint, the photodimerization of **2c** generally gives the HT-dimers as main products, because of the steric and/or electrostatic repulsion between the carboxylate moieties (Table 1, refs.). Therefore, the present exclusive HH-dimer formation is undoubtedly attributable to capability of the reaction media, which overcame the intrinsic reaction course. In the cases of the crystalline and LC phases, such a strong preference to HH-dimer formation is reasonably elucidated, assuming that (1) the matrices take a bilayer-like structure, and that (2) an intralayer dimerization is a much favorable process than an inter-layer dimerization (see Figure 3c). Noteworthy, all of the isotropic phases also afforded the HH-dimers in unexpectedly good selectivities (entries 3, 11, and 16, Iso[**1a**·**2c**], Iso[**1b**·**2c**], and Iso[**1c**·**2c**], HH:HT = 86:14–97:3), which is in contrary to a generally conceived notion that molecules take random arrangement in an isotropic phase. Because the present salts are regarded as ionic LC materials, strong interactions are likely to work between the components, which would lead to partial retention

of the molecular alignment even after the transition from a crystalline/LC phase to an isotropic phase.<sup>29</sup>

**2.5.3. syn/anti Selectivity.** As described above, main products in the present reaction systems were the syn<sup>HH</sup>- and anti<sup>HH</sup>-dimers, while the syn<sup>HT</sup>- and anti<sup>HT</sup>-dimers were formed in negligible yields. Therefore, the discussion in this section focuses on the effect of the reaction systems on syn<sup>HH</sup>/anti<sup>HH</sup> ratios.

As summarized in Table 1, the syn<sup>HH</sup>/anti<sup>HH</sup> ratio notably varied, depending on the amino alcohol unit as well as the phase. For most of the present reaction systems, slight syn<sup>HH</sup>-selectivity (syn<sup>HH</sup>:anti<sup>HH</sup> = 52:45–56:41) was observed, including all of the isotropic phases (entry 3, Iso[**1a**·**2c**]; entry 11, Iso[**1b**·**2c**]; entry 16, Iso[**1c**·**2c**]), the LC phase (entries 12 and 13, Sm<sub>X</sub>[**1c**·**2c**]), and the crystalline phase (entries 1 and 2, Cry[**1a**·**2c**]). In contrast, the following three LC phases (Meso[**1b**·**2c**], Sm<sub>A</sub>[**1b**·**2c**], and Sm<sub>A</sub>[**1c**·**2c**]) interestingly showed selectivities distinguishable from the others. Among them, Sm<sub>A</sub>[**1c**·**2c**] showed prominent syn<sup>HH</sup>-selectivity (entries 14 and 15, Sm<sub>A</sub>[**1c**·**2c**], syn<sup>HH</sup>:anti<sup>HH</sup> = 61:37). On the other hand, the two LC phases of **1b**·**2c** showed the opposite selectivity, i.e. the preferential formation of the anti<sup>HH</sup>-dimer was observed (entries 4–8, Meso[**1b**·**2c**], 28:70–26:72; entries 9 and 10, Sm<sub>A</sub>[**1b**·**2c**], 48:49–46:52). Noteworthy, the syn<sup>HH</sup>/anti<sup>HH</sup> ratio of the photodimerization product could be rationally controlled in the present reaction system, by choosing an

(29) For selected examples of multicomponent ionic liquid crystals, see: (a) Yoshio, M.; Mukai, T.; Ohno, H.; Kato, T. *J. Am. Chem. Soc.* **2004**, *126*, 994–995. (b) Cook, A. G.; Baumeister, U.; Tschierske, C. *J. Mater. Chem.* **2005**, *15*, 1708–1721. (c) Kouwer, P. H. J.; Swager, T. M. *J. Am. Chem. Soc.* **2007**, *129*, 14042–14052. (d) Kishikawa, K.; Hirai, A.; Kohmoto, S. *Chem. Mater.* **2008**, *20*, 1931–1935. (e) Olivier, J.-H.; Camerel, F.; Barberá, J.; Retailleau, P.; Ziessel, R. *Chem.–Eur. J.* **2009**, *15*, 8163–8174.



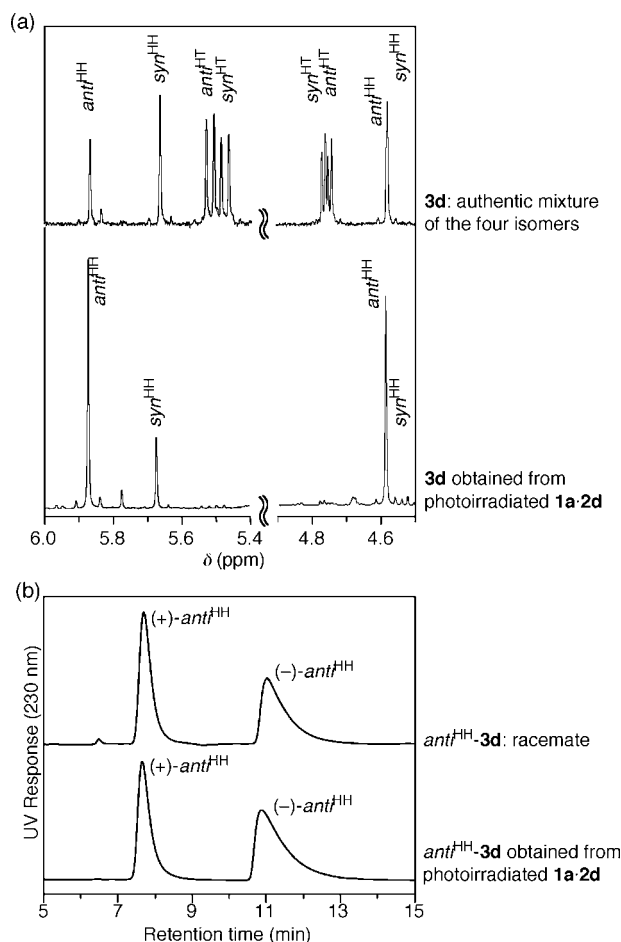
appropriate amino alcohol unit and phase. Although a number of reaction systems have been reported to control the photodimerization of **2c**, a detailed study on the control of a *syn/anti* ratio has been very limited, as far as we know.

**2.5.4. Enantioselectivity.** Among the major products provided in the present reaction systems, the *anti*<sup>HH</sup>-dimer has a C<sub>2</sub> symmetric chirality, whereas the *syn*<sup>HH</sup>-dimer is achiral. Quite interestingly, one of the two LC phases of **1b·2c** (Meso[**1b·2c**]) afforded the *anti*<sup>HH</sup>-dimer with unexpectedly high enantioselectivity (Table 1, entries 4–8, Meso[**1b·2c**], +67 to +86% ee). Even in the other LC phase of **1b·2c** at a higher thermal region (Sm<sub>A</sub>[**1b·2c**]), the enantiocontrol was also at an appreciable level, although the control was inferior to that of Meso[**1b·2c**] (entries 6 and 7, Sm<sub>A</sub>[**1b·2c**], +26 and +48% ee). As far as we know, the enantiocontrol achieved in Meso[**1b·2c**] is the second highest in the asymmetric photodimerizations of **2c** having been reported to date.<sup>24c</sup> The present outstanding selectivity was not a simple chirality transfer within the discrete salt pair, but was a result driven by the framework of the chiral supramolecular architecture, because the isotropic phase attained only insufficient selectivity (entry 11, Iso[**1b·2c**], +18% ee). In the case of **1c·2c**, the LC phase at a lower thermal region (Sm<sub>X</sub>[**1c·2c**]) showed relatively good enantioselectivity (entries 12 and 13, Sm<sub>X</sub>[**1c·2c**], ~30% ee), while the other LC phase (Sm<sub>A</sub>[**1c·2c**]) afforded the *anti*<sup>HH</sup>-dimer with moderate enantioselectivity (entries 14 and 15, Sm<sub>A</sub>[**1c·2c**], ~+15% ee), comparable to that of the isotropic phase (entry 16, Iso[**1c·2c**], 13% ee). Contrary to our expectation, the crystalline phase of **1a·2c** showed unsatisfactory enantioselectivity (entries 1 and 2, Cry[**1a·2c**], ~-15% ee); most likely, the photodimerization proceeded mainly at defects in the crystal, so that the selectivity would not necessarily reflect the highly ordered structure in the crystal.

Concerning the preference of the stereochemical outcomes, worth noting is that the stereochemistry of the major enantiomer was perfectly correlated with that of the stereogenic carbon adjacent to the hydroxy group (C1) in the amino alcohol unit; **1b** (C1: *S*) and **1c** (C1: *S*) afforded the (+)-*anti*<sup>HH</sup>-dimer, whereas **1a** (C1: *R*) gave the (-)-*anti*<sup>HH</sup>-dimer. In other words, the absolute configuration of the preferentially produced *anti*<sup>HH</sup>-dimer might be 'predictable' from the C1 stereochemistry of the amino alcohol unit.

**2.6. Photodimerization of 1-Anthracenecarboxylic Acid (2d) in the Amphiphilic Salts.** We next performed the in situ photodimerization of 1-anthracenecarboxylic acid (**2d**) in the reaction systems composed of the salts with **1a–c**. The photodimerization and product analyses were carried out by using procedures similar to those of **2c**; the photoirradiated sample was subjected to thorough esterification, and the yield, isomer distribution, and enantiomeric ratio of the photodimer diesters **3d** were evaluated. The ratio of the four isomers (*syn*<sup>HH</sup>, *anti*<sup>HH</sup>, *syn*<sup>HT</sup>, and *anti*<sup>HT</sup>-isomers) was determined by <sup>1</sup>H NMR without resorting to a HPLC analysis; <sup>1</sup>H NMR signals attributable to the bridge-head methyne protons of the four isomers were observed separately from each other (Figure 5a). The results are summarized in Table 2.

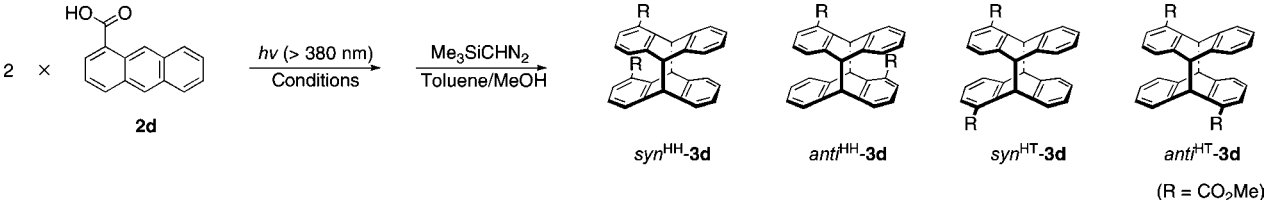
**2.6.1. Reactivity.** In all of the reaction systems, the photodimerization of **2d** proceeded cleanly to give a mixture of the photodimers in acceptable to good yields (Table 2, entries 1–7, 36–77% yield). The only detectable side reaction was the formation of an anthraquinone derivative, which was similar to the case of the systems containing **2c**. Overall, the yields of the photodimers of **2d** were lower than those of **2c** to some extent.



**Figure 5.** (a) Estimation of the isomer distribution by <sup>1</sup>H NMR. An authentic mixture of the four isomers of **3d** (top) and a mixture obtained from photoirradiated **1a·2d** (bottom). (b) Estimation of the enantiomeric ratio of *anti*<sup>HH</sup>-**3d** by chiral HPLC. An authentic racemate of *anti*<sup>HH</sup>-**3d** (top) and *anti*<sup>HH</sup>-**3d** obtained from photoirradiated **1a·2d** (bottom).

Even in the isotropic phases, the photodimerization proceeded only at a moderate level to achieve 57–77% yield (entries 2, 4, and 7, Iso[**1a·2d**], Iso[**1b·2d**], and Iso[**1c·2d**]). These results indicate that the reactivity of **2d** in the salts with **1a–c** is a little lower than that of **2c** in its salts. On the other hand, the crystalline phases of **1a·2d** and **1b·2d** surprisingly achieved acceptable yields (entry 1, Cry[**1a·2d**], 55% yield; entry 3, Cry[**1b·2d**], 39% yield), which were comparable to that of the LC phase of **1c·2d** (entries 5 and 6, Sm<sub>A</sub>[**1c·2d**], up to 43% yield).

**2.6.2. HH/HT Selectivity.** In all of the present reaction systems, the photodimerization of **2d** commonly proceeded in a highly HH-selective manner (HH:HT = 81:19–99:1). Most likely, the same mechanism, as was considered for the reaction of **2c**, worked in the photodimerization of **2d**; within a bilayer-like structure, an *intra*-layer dimerization proceeded much faster than an *inter*-layer dimerization. Worth noting is that the LC phase of **1c·2d** (Sm<sub>A</sub>[**1c·2d**]) showed extremely high HH-selectivity, where the HT-dimer was not detected at all by <sup>1</sup>H NMR (entries 5 and 6, Sm<sub>A</sub>[**1c·2d**], HH:HT = >99:1). The HH/HT selectivity achieved here was the highest in the present study, including the photodimerization of **2c**. Unexpectedly, the isotropic phases (Iso[**1a·2d**], Iso[**1b·2d**], and Iso[**1c·2d**]) again showed relatively high HH-selectivity, probably because the isotropic phases partially retained a structural order similar to

**Table 2.** Photodimerization of 1-Anthracenecarboxylic Acid (**2d**)<sup>a</sup>


entry	medium	phase	temp. (°C)	time (h)	yield (%) <sup>b</sup>	product ratio (%) <sup>c</sup>				ee (%) <sup>d</sup> anti <sup>HH</sup>
						syn <sup>HH</sup>	anti <sup>HH</sup>	syn <sup>HT</sup>	anti <sup>HT</sup>	
1	<b>1a</b>	Cry	25	15	55	75	22	2	2	-13
2		Iso	100	3	72	69	24	4	4	10
3	<b>1b</b>	Cry	25	15	39	47	40	10	3	-6
4		Iso	90	3	57	50	30	11	8	-8
5	<b>1c</b>	Sm <sub>A</sub>	65	3	36	67	33	<1	<1	-9
6		Sm <sub>A</sub>	65	15	43	66	34	<1	<1	-5
7		Iso	120	3	77	57	34	5	5	n.d.

<sup>a</sup> Irradiated at  $\lambda = >380$  nm under argon. <sup>b</sup> Determined by <sup>1</sup>H NMR. <sup>c</sup> Isomer distribution of **3d** estimated by achiral HPLC. <sup>d</sup> Enantiomeric excess of anti<sup>HH</sup>-**3d** estimated by chiral HPLC. The signs + and - represent that the major product was the first- and second-eluted enantiomer in the chiral HPLC analysis, respectively.

those of the LC/crystalline phases (entries 2, 4, 7, Iso[**1a**·**2d**], Iso[**1b**·**2d**], and Iso[**1c**·**2d**], HH:HT = 81:19–92:8).

Taking into account of the results of the photodimerizations of the two substrates **2c** and **2d**, we can clearly conclude that the present amphiphilic salts generally promote HH-dimer formation; in both cases, the reaction media strongly directed the reaction course to exclusively afford the HH-dimers, in spite of their thermodynamically disadvantageous structures.

**2.6.3. syn/anti Selectivity.** Without depending on the amino alcohol unit or the phase, the syn<sup>HH</sup>-dimer was generally afforded as a predominant product. Although similar syn<sup>HH</sup>-selectivity was also observed in the case of the reactions of **2c**, the photodimerization of **2d** showed this tendency more markedly. Particularly, the crystalline phase of **1a**·**2d** realized a syn<sup>HH</sup>/anti<sup>HH</sup> ratio of no less than 75:22. Such a strong syn<sup>HH</sup> preference in the photodimerization of **2d** probably originated from a self-assembled structure based on a hydrogen-bonding network together with the characteristic structures of the photodimers of **2d**. In the amphiphilic salts, a one-dimensional hydrogen-bonding network of the functional groups (carboxylate, ammonium, and hydroxy) is considered to be formed, which would force carboxylate groups to be located near each other. Since such a ground-state orientation should be reflected on its excited-state orientation, the formation of the anti<sup>HH</sup>-dimer of **2d**, of which the two carboxylate groups are located apart from each other, is considered to be unfavorable, compared with that of the syn<sup>HH</sup>-dimer.

**2.6.4. Enantioselectivity.** Among the photodimers of **2d**, the anti<sup>HH</sup>- and syn<sup>HT</sup>-dimers have a C<sub>2</sub> symmetric chirality, while the other two dimers are achiral. Due to the perfect HH selectivity of the present reaction systems, we focused on the anti<sup>HH</sup>-dimer as a target product in the context of enantiocontrol. Unfortunately, however, all of the amphiphilic salts afforded the anti<sup>HH</sup>-dimer as the second major product. In addition, the ee value of the anti<sup>HH</sup>-dimer generated here was encouraging, but far from an ideal level (up to -13% ee). For the preference of the stereochemical outcomes, the configuration of the C1 in the amino alcohol unit was again found to be a determinant factor; in general, the amino alcohols with (*S*)-configuration at the C1 position generated the (-)-anti<sup>HH</sup>-dimer, although the only exceptional result was obtained when the reaction was carried out in the crystalline phase of **1a**·**2d** (entry 3,

Cry[**1a**·**2d**]). Overall, the enantiocontrol of the anti<sup>HH</sup>-dimer formation of **2d** was at an unsatisfactory level, compared with that of the reaction of **2c**. Because of a relatively large distance between the two carboxylate groups in the anti<sup>HH</sup>-dimer of **2d**, we may need to design another amino alcohol unit for the improvement of the enantioselectivity.

**2.7. Mechanistic Aspect I: Stereochemistry and Conformational Preference of the Amino Alcohols.** The results mentioned above clearly show that the stereochemistry of the amino alcohol unit brought significant effects on the properties of their salts, such as the thermal behavior, self-assembled structure, and capability of controlling the in situ photoreaction. Worth noting is that such a subtle modification around the C1/C2 positions was a determinant for these properties. For further sophisticated design of an amino alcohol unit, it might be important to elucidate the relationship between the substitution pattern and the three-dimensional structure of the amino alcohol units. Thus, we examined the Cambridge Structure Database (CSD) for the salts of analogous amino alcohols with acids. We searched for structures containing the fundamental skeleton of erythro-2-amino-1-phenyl-1-propanol (type **a**), threo-2-amino-1-phenyl-1-propanol (type **b**), and 2-amino-1-phenylethanol (type **c**), as the analogues of **1a**, **1b**, and **1c**, respectively (Figure 6a), to give a total of 22 structures (type **a**, 10 structures; type **b**, 2 structures; type **c**, 10 structures).<sup>30</sup>

In principle, three kinds of rotamers are possible for the present amino alcohols (AG, GG, and GA); the first and second indices (G, *gauche*; A, *anti*) represent the arrangement of the C(Ar)-C1-C2-N and O-C1-C2-N chains, respectively (Figure 6b).<sup>31c</sup> Among the 22 structures retrieved from CSD, 20 structures were found to take an AG conformation. Therefore, we can conclude that the present amino alcohols have a strong tendency to take an AG conformation.<sup>31</sup> In order to simplify

(30) Crystal structures with the following CSD entry codes were used. Type **a**: amagaw, jastus, mixpeac, nephcl, qawsuc, ugeyua, vejgeg. Type **b**: geveeb, jasvaa. Type **c**: cektuh, cimkeo, hpetic, jammal, nadren, nadrhc, octopc, yivcem, yvcig, yivcow.

(31) For the conformational behavior of norephedrine and derivatives, see: (a) Pullman, B.; Coubeils, J. L.; Courriere, P.; Gervois, J. P. *J. Med. Chem.* **1972**, *15*, 17–23. (b) Tsai, H.; Roberts, J. D. *Magn. Reson. Chem.* **1992**, *30*, 828–830. (c) Alonso, J. L.; Sanz, M. E.; López, J. C.; Cortijo, V. *J. Am. Chem. Soc.* **2009**, *131*, 4320–4326.

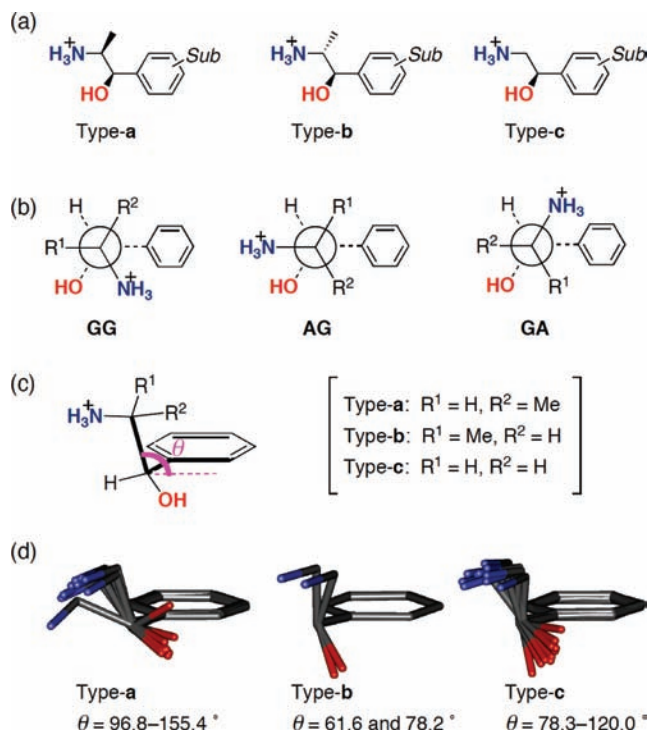


**Figure 6.** (a) Three types of amino alcohols as analogues of **1a–c**. *Sub* represents the substituent(s) on the aromatic ring. (b) Newman projections of the possible conformers of the present amino alcohols. (c) Definition of the dihedral angle  $\theta$ . (d) Superimposition of structures retrieved from CSD. Hydrogen atoms, C2-methyl groups, and substituent(s) on the aromatic ring are omitted for clarity.

comparison, only the structures taking an AG conformation were adopted in the following discussion.

In the cases of amino alcohols bearing a C2-methyl group (type **a** and type **b**), an AG conformation should cause considerable steric hindrance between the methyl and aromatic groups. As a result, the aromatic group is anticipated to tilt in the direction opposite the methyl group. On the other hand, the aromatic group in type **c** amino alcohols seems to be able to take various orientations. To confirm the anticipation, the dihedral angle  $\theta$ , as defined in Figure 6c, was calculated on the basis of the structures obtained from CSD. As might be expected from the orientation of the C2-methyl group, the dihedral angles of type-**b** amino alcohols ( $\theta = 61.6$  and  $78.2^\circ$ , Figure 6d, middle) were obviously smaller than those of type-**a** amino alcohols ( $\theta = 96.8\text{--}155.4^\circ$ , Figure 6d, left). Meanwhile, type-**c** amino alcohols were found to take a wide range of  $\theta$  ( $78.3\text{--}120.0^\circ$ , Figure 6d, right), most likely because this type of amino alcohols has almost no steric hindrance. For further confirmation, theoretical calculations at the HF/6-31G level were conducted for these three types of amino alcohols, which showed a tendency similar to that of the CSD studies; the dihedral angles  $\theta$  of the optimized structures were  $90.0$ ,  $70.8$ , and  $73.2^\circ$  for type **a**, **b**, and **c**, respectively. Since the dihedral angle  $\theta$  directly reflects the relative orientation of the amino/hydroxy groups and the aromatic ring, it is quite reasonable that the salts of **1a–c** showed different characteristics as described above. Thus, the stereochemistry at C1 and the substituent at C2 of the amphiphilic amino alcohols play a very important role to determine their characteristics, although it is generally accepted that the self-organization of amphiphilic molecules can be simply elucidated on the basis of a hydrophilic–hydrophobic volume ratio. Although there are still some unclear points, further

modification of the amino alcohol unit, such as the replacement of the methyl group in **1a** or **1b** with a bulkier substituent, would be attractive.

**2.8. Mechanistic Aspect II: “Topotacticity” of the Two-Component LC Reaction System.** The present photoreactions of two-component LCs generally showed unprecedentedly high HH/HT selectivity even after achieving high conversion (HH: HT = 97:3 to 99:1), regardless of the choice of amino alcohol and carboxylic acid units. Such generality, i.e. the tolerance toward variation in the shape of components, might be one of the most outstanding benefits, compared with that of the reactions in the crystalline state. Within the framework of traditional crystalline-state reaction systems, “topotacticity” is a determinant factor for the reactivity and selectivity. In the case of topochemical systems, the difference between substrates and products is so small that the original three-dimensional order is preserved with relatively small adjustments in the unit cell. On the other hand, solid-to-solid reconstructive systems involve sufficiently large molecular movement, which leads to the complicated changes of crystalline lattice. Therefore, it is worthwhile to investigate the structural changes during the present reactions, which would give a clue to elucidate the origin of the general versatility of our LC reaction system.

As a model system, we chose the  $Sm_X$  phase of **1c·2c** ( $Sm_X[1c·2c]$ ), because of its simple XRD pattern, as well as its wide thermal window ranging over rt. The salt **1c·2c** was irradiated at  $20^\circ\text{C}$  for 15 h ( $\sim 80\%$  conversion of **2c** into the photodimers), and the changes before and after irradiation were investigated by XRD, POM, and DSC. As depicted in Figure 7a, 15-h irradiation caused no distinct change in the XRD pattern, where a strong reflection was observed at a small-angle region assignable to (001), accompanied with a diffuse reflection at a wide-angle region due to the loose packing of the paraffin moiety. A closer comparison of these XRD patterns revealed that the *d*-spacing calculated from the (001) reflection increased from 30 to 33 Å. In POM observation, the focal conical texture of the original state was retained throughout the photoreaction, which also indicates that a drastic phase transition was not likely to happen during the in situ photoreaction. Moreover, DSC and variable-temperature POM revealed that the irradiated sample acted as a thermotropic LC; through the scanning between  $-50$  and  $150^\circ\text{C}$ , the irradiated salt exhibited a LC phase in both of the cooling and heating processes.<sup>32</sup>

These observations strongly suggest that (1) the fundamental structure of the smectic LC was retained through the photodimerization, and (2) the photodimerization induced a remarkable change in the layer distance ( $\sim 10\%$  increase). Supposing that density of the salt is essentially unchanged during the photoreaction-induced transformation, the increase in  $d_{(001)}$  might be elucidated as follows; because the photodimerization should decrease the averaged distance between the carboxylate groups, the structural unit would shrink in the *z*-axis direction. As compensation, the unit would expand in the *x*-axis direction by reducing the degree of interdigitation of the tail parts, in order to avoid the congestion of the alkyl chains (Figure 7b). Most likely, such a flexible nature enabled the present LC system to suppress the collapse of the original smectic structure. As a result, the high HH selectivity would be achieved even at the

(32) Generally, the photodimers of anthracene derivatives are known to undergo thermal cleavage to afford the monomer when extensively heated. In the case of the present LC salt obtained by the irradiation of **1c·2c**, however, the cleavage of the photodimer **3c** did not proceed at a detectable level through the present DSC measurement.



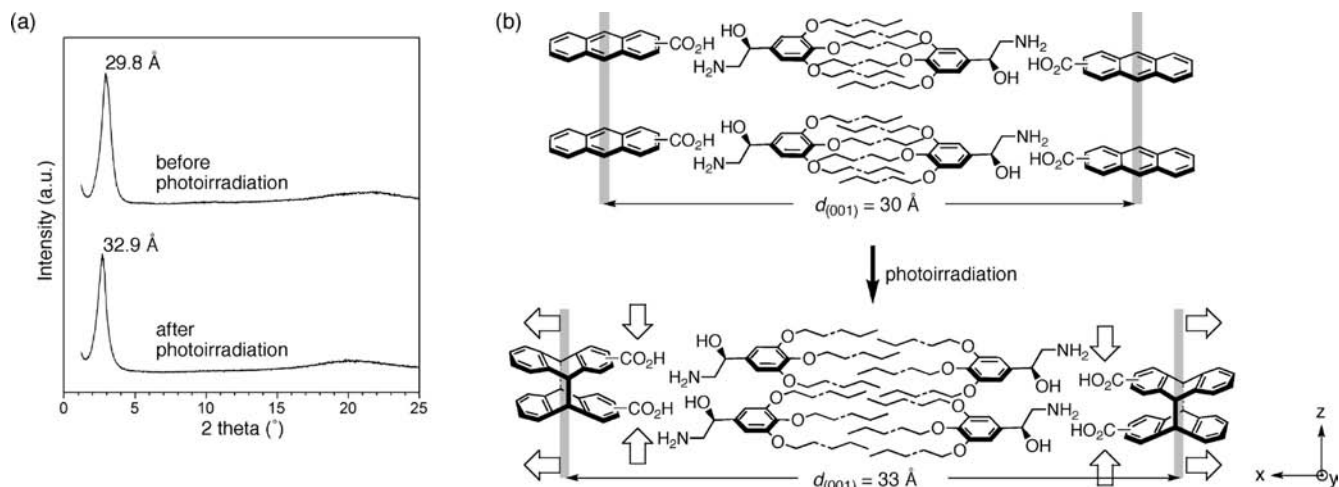


**Figure 7.** (a) XRD pattern of **1c·2c** before (top) and after (bottom) photoirradiation ( $\lambda > 380$  nm under argon, at 20 °C for 15 h). (b) Schematic representation of the plausible structural changes of **1c·2c** through the photodimerization of **2c**. Blank arrows represent the transformation of the lattice.

last stage of this photoreaction, where most of the starting materials had been converted.

### 3. Conclusion

We have demonstrated that two-component liquid crystals, composed of the salts of enantiopure amphiphilic amino alcohols with anthracenecarboxylic acids (**2c**: 2-anthracenecarboxylic acid, **2d**: 1-anthracenecarboxylic acid) generally offer a unique reaction environment for the photodimerization of the carboxylic acid unit. Three types of amino alcohols were developed, of which the stereochemistry around the amino and hydroxy groups was systematically varied (stereochemistry of C1/C2: **1a** *R/S*, **1b** *S/S*, and **1c** *S*/achiral). On a cooling process from an isotropic melt, some combinations exhibited one or two kinds of LC phases (**1b·2c**, **1c·2c**, and **1c·2d**), while the other (**1a·2c**, **1a·2d**, and **1b·2d**) showed direct transition into a crystalline phase. In every LC phase obtained here, the photodimerization of the carboxylic acid unit proceeded efficiently with excellent selectivity, which strongly suggests the general utility of the two-component liquid crystal method. Moreover, the choice of the amino alcohol unit and the phase brought a notable effect on the isomer distribution of the photoreaction product. In other

words, these three amino alcohols might play a complementary role to each other, and therefore, the present work has certainly expanded the scope of this method. As far as we are aware of, the present LC system is one of the most advantageous reaction media to direct the photodimerization of anthracenecarboxylic acids, from the viewpoints of generality, simplicity, reactivity, regio-/diastereo-/enantioselectivities, and tunability. By using the synthetic method established here, various amphiphilic amino alcohols would be available in stereopure forms, which would further expand the scope of the present methodology.

**Acknowledgment.** We acknowledge Dr. Toshimi Shimizu and Dr. Hiroyuki Minamikawa (AIST), for XRD measurements.

**Supporting Information Available:** Synthesis and characterization of the amphiphilic amino alcohols **1a–c**, preparation and thermal behavior of the 12 kinds of salts **1·2**, experimental details for the photodimerization of the anthracenecarboxylic acids **2c** and **2d**, and X-ray crystallographic data for the salt of (*R*)-**11** with (*S*)-mandelic acid. This material is available free of charge via the Internet at <http://pubs.acs.org>.

JA105221U